

THE INFLUENCE OF HYDRODYNAMIC FORCING ON SEDIMENT TRANSPORT PATHWAYS AND SHORELINE EVOLUTION IN A CORAL REEF ENVIRONMENT

Andrew WM Pomeroy¹, Ryan J Lowe¹, Carlin Bowyer², Zhenlin Zhang¹, James Falter¹,
Ap Van Dongeren³, Dano Roelvink^{3,4,5}

Abstract

Fringing coral reef systems shape the dominant hydrodynamic processes that transport sediment within these environments which, over long time scales, can lead to the formation of various major planform (horizontal) morphological features. In this study, the influence of reef morphology on hydrodynamic processes within a coral reef environment was investigated in a field experiment conducted at Coral Bay (Ningaloo Reef, Western Australia) with the aim to identify sediment transport paths that are likely to affect the evolution of the adjacent shoreline. The shoreline position at the site was analyzed to identify net shoreline movements over an ~60 year period of digitized aerial photography. The sediment characteristics varied throughout the site with extensive regions of relatively coarser (1.1 – 1.3 Φ) sediment generally associated with areas with high coral coverage, some isolated regions of moderately coarse sediment and three large regions of relatively finer sediment (2.2 – 1.8 Φ) that were typically associated with large, un-colonized sandy patches. Whilst the position of coastline was largely stable (< 0 – 10 m movement) over the ~60 years of shoreline data available, substantial migrations (~ 30 – 150 m) were observed along isolated sections of coastline. The numerical model XBeach was used to model the reef and lagoon hydrodynamics from which two types of flow were identified: (1) several hydrodynamic circulation cells that are isolated from adjacent cells and (2) an interconnected cell system whereby an alongshore current propagates along the coastline and between cells before it empties into a large bay to the north of the site. Acceleration of flow adjacent to cusped forelands and an absence of feature development suggest that some of these features are in a state of equilibrium, while the flow separation around Point Maud and the presence of a persistent eddy at this location is likely to be associated with the continual accretion of this feature over the study period.

Key words: sediment, hydrodynamics, morphology, coral reefs

1. Introduction

The development of planform features along a coastline adjacent to a fringing coral reef involves complex interactions between the production of sediment, its transport by hydrodynamic processes and its patterns of deposition. Over long time scales, various major coastline features such as cusped forelands and salients have been observed to develop adjacent to both fringing tropical coral reefs and temperate bedrock reefs (e.g. Sanderson, 2000; Sanderson and Eliot, 1996). However, in order to accurately model the development of these features, the regulation of sediment production and transport pathways within reef environments must first be understood. This is not trivial due to the presence of a complex coral framework that is not only a major source of sediment production but also a substantial determinant of hydrodynamic variability across reef systems as well as how sediments are transported.

The production and reworking of sediment in reef environments is a balance between constructive and destructive physical, biological and chemical processes (e.g. Scoffin, 1992) as well as differences in the ecological state of a reef (Done, 1992). The continual incorporation of calcium carbonate into reef frameworks produced by coral calcification (Vecsei, 2004), as well as other sources such as crustose

¹The University of Western Australia, School of Earth and Environment and The UWA Oceans Institute, 35 Stirling Highway, Crawley, 6009, Australia.

²MScience Pty Ltd, 99 Broadway, Nedlands, 6009, Western Australia, Australia

³Deltares, Dept. ZKS and HYE, P.O. Box 177, 2600 MH, Delft, The Netherlands

⁴UNESCO-IHE, P.O. Box 3015, 2601 DA, Delft, Netherlands

⁵Delft University of Technology, P.O. Box 5048, 2600 GA, Delft, The Netherlands

coralline algae (Perry and Hepburn, 2008), construct reef environments. Calcium carbonate becomes mobilized as sediment by destructive processes (e.g., by bio- and mechanical erosion) that act to degrade these frameworks over time (Scoffin, 1992). The resulting carbonate sediment, possibly along with external sediment sources such as terrestrial runoff (Ogston et al., 2004; Presto et al., 2006; Storlazzi et al., 2004) and alongshore sediment transport, can then be exported away from actively growing regions of the reef where they may be deposited to form coastline features.

The steep forereef slope and wide shallow reef flat that typically characterize coral reefs regulate the hydrodynamic conditions on the reef and within the lagoon (Monismith, 2007). Incident waves break on the shallow reef crest (Hardy and Young, 1996; Young, 1989) and energy is dissipated and redistributed to both higher and lower frequencies (Lee and Black, 1978; Pomeroy et al., 2012). Wave forces (radiation stress gradients) establish wave setup variations (and consequently a pressure gradient) that drives currents across the reef and forces circulation through the lagoon before it returns to the ocean via channels that typically perforate the reef structure (Lowe et al., 2009; Taebi et al., 2011). The high bottom roughness of reefs (i.e. as formed by coral reef communities) induce frictional dissipation of these hydrodynamic processes with frictional coefficients that are up to an order of magnitude greater than those estimated for sandy beach environments (Lowe et al., 2005c; Pomeroy et al., 2012; Rosman and Hench, 2011; Van Dongeren et al., 2013). While considerable advances have been made in our understanding of hydrodynamic processes on reefs, the connection with sediment pathways and consequently coastal morphodynamics is still not well understood.

In this study we present the results of a field study that included the collection of hydrodynamic and sediment data, in order to understand the distribution of different sediment characteristics throughout a fringing coral reef and their relationship to hydrodynamic forcing. Analysis of long-term (~60 years) of digitized shoreline data is then used to understand how the presence of the reef structures influence contemporary shoreline changes, including quantifying regions of accretion and erosion. We then use the numerical model XBeach to simulate the dominant hydrodynamic processes at the site. The implications of the hydrodynamic circulation patterns and bed shear stress distributions on the dominant sediment transport pathways, as well as their role in regulating shoreline development, are then discussed.

2. Methods

2.1 Site description

The field experiment was conducted at Coral Bay (23° 08' S, 113° 45' E, Figure 1), in the southern section of Ningaloo Reef in Western Australia. The specific study region was bounded by Point Maud and North Passage to the north (which connects this section of reef to the larger reef-fringed Bateman Bay) and Point Anderson in the south. The reef that fringes this section of coastline has a number of channels, with the most prominent being North Passage in the north and False Passage in the north-west. A number of smaller channels also permit the return of wave-driven flow along this section of reef (Figure 1). The reef flat is ~0.6 – 1.5 m below mean sea level and typically ranges between ~300 to 800 m in width. The lagoon is generally ~3 m deep and is connected with deeper channels that are up to ~6 m deep; it also varies in width along the coast. Coral coverage at Coral Bay is extensive (~40 % inside the lagoon to ~90 % at the outer reef margin) and is primarily populated by species of *Acropora* and *Montipora* (Wyatt et al., 2010).

2.2 Field experiment

The field experiment was conducted during the 2010 austral winter (4th – 14th July). Zhang et al. (2012) describes the full experiment and only a brief summary of the key hydrodynamic aspects of the experiment relevant to the present study are presented here.

A 1 MHz Nortek AWAC current profiler/directional wave gauge was deployed on the forereef (S1, Figure 1). Surface water elevations were measured by acoustic surface tracking at 1 Hz and current profiles with a bin size of 0.5 m were measured every five minutes. On the reef flat (S2, Figure 1) a 2 MHz Nortek AquaDopp profiler (ADP) measured current profiles with high vertical resolution (0.1 m) every 15 minutes. The flow within the lagoon was measured every 15 minutes with a 0.15 m vertical resolution with

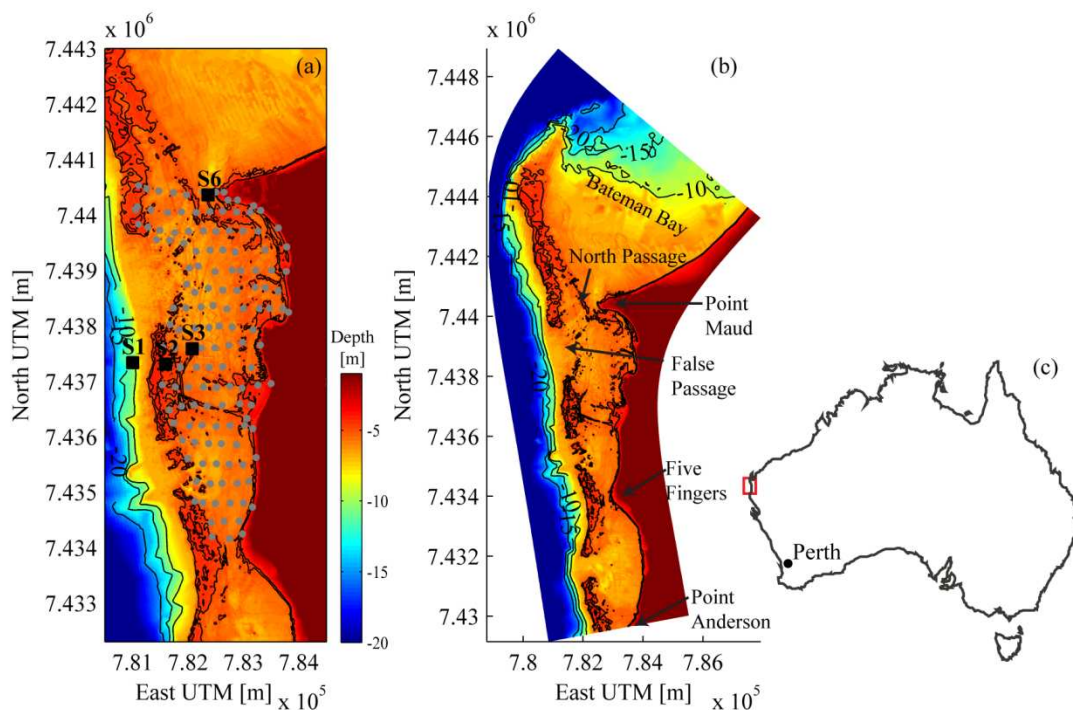


Figure 1. (a) Study site at Coral Bay with the locations of sediment grab samples (grey circles) and the location of hydrodynamic instruments (black squares). (b) Some key morphological features of Coral Bay. The depth of the bathymetry is indicated by the color bar. (c) Location of Coral Bay within Australia.

a 1200 kHz RD Instruments ADCP (S3, Figure 1) and the flow out of the lagoon via the North Passage was measured every 15 minutes with a 600 kHz RD Instruments ADCP deployed in the center of the channel (S6, Figure 1) with a 0.3 m bin size. Table 1 summarizes the instrument locations and sampling configurations.

Wave spectra $S_{\eta\eta}$ were estimated for each hourly burst of data by computing the spectral density of the water surface elevation fluctuations η measured directly by the AWAC AST. The spectra were computed using a Welch's averaged modified periodogram, with 50% overlap and Hanning windows applied, to reduce spectral leakage. From these wave spectra, the hourly root mean squared (rms) wave heights H_{rms} , peak periods T_p , and peak wave directions D_p were computed.

A staggered array of 156 sediment samples was obtained by taking surface grab samples ($\sim 0 - 7$ cm below the bed) on a regular grid (~ 200 m in the cross shore direction, ~ 350 m in the along shore direction) during the field experiment (Figure 1a). The samples were carefully collected manually by divers in 250 ml jars and capped immediately (at the bottom during the dive) to retain fine particles. The collection of surface samples enabled the sediment directly exposed to the prevalent near-bed shear stresses to be compared to the wave conditions observed during the experiment. The sediment samples were analyzed in the laboratory at The University of Western Australia to determine the sediment composition and characteristics. A 2.20 m settling tube was used to determine the cumulative rate of sediment deposition, which was then converted to an equivalent spherical grain size distribution following Gibbs et al. (1971). The characteristics (e.g. mean, sorting, skewness, kurtosis) of the distributions were then quantified.

2.3 Shoreline change analysis

Historical shoreline changes were quantified with aerial photography (1949 to 2008) using the Digital Shoreline Analysis System (Thieler et al., 2008) in ArcGIS. The images ($n = 25$) were rectified by resampling the original image to a new coordinate system using a cubic convolution and control points defined on a previously geo-rectified 2002 Coral Bay – Exmouth Mosaic with ~ 1.4 m pixel resolution.

Local accuracy was preserved by use of spine transformation to rubber sheet the images. The shoreline position in the rectified images was digitized manually and was defined from the vegetation line (Moore, 2000; Thieler et al., 2008). The digitized shoreline positions for each year were then subjected to a digital shoreline analysis from which the net shoreline change was estimated. The root mean squared error (rmse) associated with the rectification and analysis method was calculated by using 20 randomly distributed locations from which the Euclidian distance between that point in the target and reference images were determined. The uncertainty associated with pixel resolution in the images (<0.8 m) and from the identification of the shoreline was quantified and included in the error analysis. Newer images (since 1970) were found to have a root mean squared position error of less than 4 m. Images from the 1960's were found to have an rms error of ~4.3 m while the oldest set of images (1949) had an error of ~9 m.

Table 1. Instrument site information and sampling configuration

Site	Depth (m)	Instrument	Sampling Information
S1 (forereef)	12.7	Nortek 1 MHz AWAC	1 Hz with 2048 s burst every 3600 s; velocity profiles every 300 s in 0.5 m bins. Instrument located 0.3 m from the bed.
S2 (reef flat)	1.3	Nortek 2MHz ADP	Velocity profiles every 900 s in 0.1 m bins. Instrument located 0.1 m from the bed.
S3 (lagoon)	3.1	1200 kHz RDI ADCP	Velocity profiles every 900 s in 0.1 m bins. Instrument located 0.3 m from the bed.
S6 (northern channel)	7.8	600 kHz RDI ADCP	Velocity profiles every 900 s in 0.3 m bins. Instrument located 0.5 m from the bed.

2.4 Numerical modeling

Hydrodynamic processes at the site were simulated with the numerical model XBeach (Roelvink et al., 2009), which was validated against hindcast simulations of the data obtained during the experiment. The focus of this initial numerical study was not on the direct simulation of sediment transport and morphodynamics but instead concentrated on understanding how sediment properties, combined with shear stress distributions, can explain erosional and depositional patterns along a coastline fringed by a coral reef. The bathymetry of the model was interpolated onto a variable curvilinear grid that extended from Bateman Bay in the north to Point Anderson in the south. The grid cell sizes ranged from ~50 m offshore of the reef to ~10 m in the lagoon. High-resolution bathymetry (3.5 m horizontal) derived from hyperspectral imagery with less than 10% rms depth error was interpolated onto the grid in the shallow regions of the domain (< 8 m) while lower-resolution boat sounding data provided by the Western Australia Department of Transport (200 m horizontal) with less than 0.2 m depth error was interpolated onto the grid in the deeper regions of the domain (> 8 m).

A coral habitat map was parameterized with coral communities represented using a hydraulic roughness parameter and implemented in the model as a variable bed friction overlay. The XBeach model simulates the dynamics of short period waves (e.g., swell waves) and long period motions (including both infragravity waves and mean currents) separately; therefore, different bed friction parameters were used to account for the frequency-dependent differences in dissipation for these types of motion. In this study we used the same parameter values that were derived in a detailed hydrodynamic modeling study that was undertaken at Sandy Bay in Ningaloo Reef (located ~100 km north of the present site) which was also conducted with XBeach (Van Dongeren et al., 2013). These include a short-wave friction factor for swell over the coral substrate ($f_w = 0.6$), a friction coefficient for low frequency / mean currents over coral ($c_f = 0.05$) that was reduced over sand patches ($c_f = 0.003$).

Current vector fields were computed for the model domain to determine the magnitude and direction of the mean flow paths around the site. The bed shear stress calculated in the model (Eqs. 0.21 and 0.22 in Roelvink et al. (2009) was used to determine the forces applied by the hydrodynamic processes on the bed sediment. These forces were compared to the critical bed shear stress (τ_{cr}) required to mobilize the bed sediment samples obtained in the experiment. The critical bed shear stress was estimated by substitution of

the critical Shield's parameter (θ_{cr}) estimated following Soulsby and Whitehouse (1997) into the non-dimensional Shield's equation with a constant sediment density equivalent to Aragonite ($\rho = 2830 \text{ kg m}^{-3}$). We use this approach as the Soulsby and Whitehouse (1997) equation follows the Shield's curve reasonably well and enables calculation of the critical Shield's parameter directly from the spatially variable mean sediment size obtained from the observations.

3. Results

3.1 Hydrodynamic field data

A broad range of wave heights were measured during the field experiment (Figure 2a). The first five days of the experiment were characterized by low waves ($H_{rms} = \sim 0.65 \text{ m}$) before a storm event occurred on the 9th July when the wave height increased over a 12 hour period to a maximum height of $\sim 3 \text{ m}$. The wave heights then decreased over the subsequent three days. The peak period of the waves was consistently within the range of 10 to 14 seconds, with the exception of the storm event where the waves decreased in period to a minimum of 5.5 s (Figure 2b). The wave direction fluctuations were minimal and approached

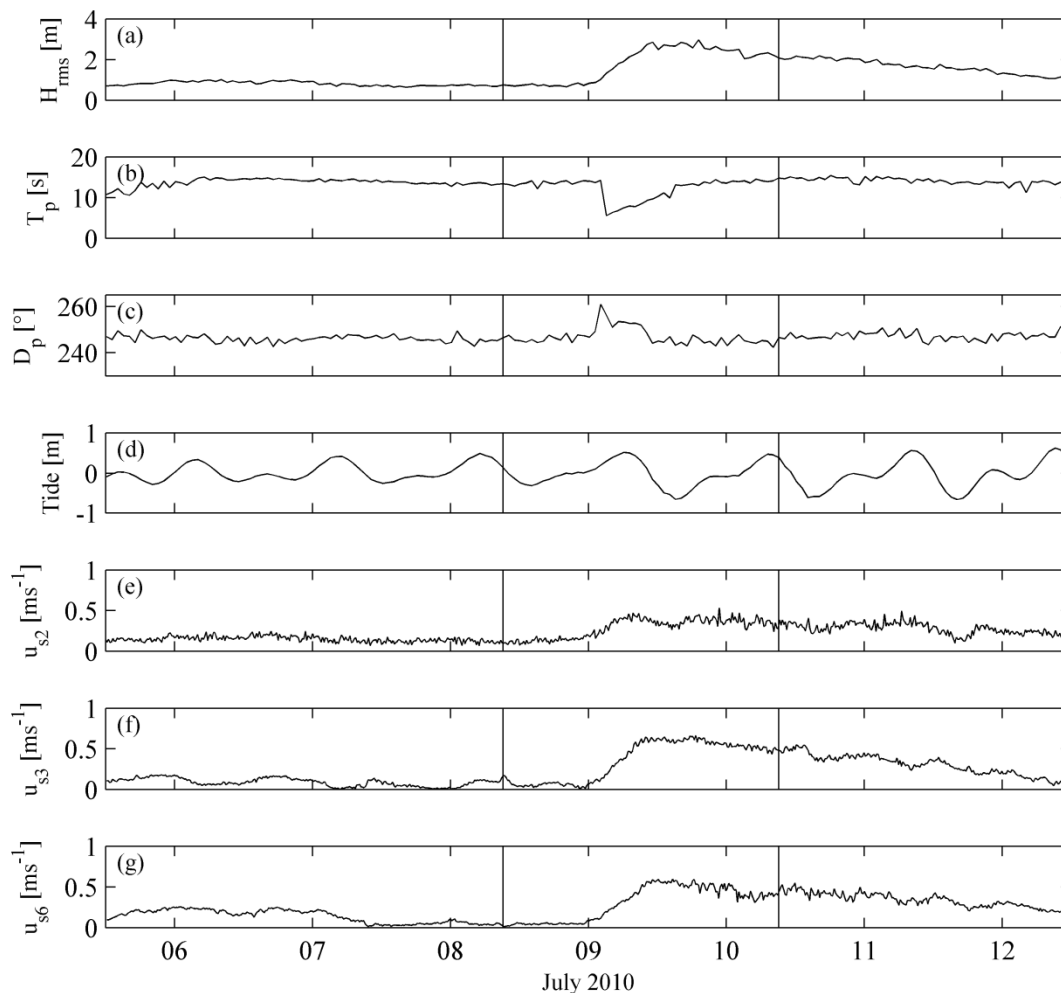


Figure 2. Hydrodynamic measurements obtained in the field experiment. The vertical lines denote the period considered in the numerical model component of this study. (a) Root Mean Squared wave height, (b) peak wave period, (c) peak wave direction and (d) tidal elevation measured on the forereef at S1. (e-g) Depth averaged velocity magnitude for the three sites in the reef (S2, S3, S6), respectively.

the reef consistently at an angle of $\sim 245^\circ$ (10° off the cross-reef direction, 255° , Figure 1) except during the storm event where the wave direction shifted to 260° before it returned to the dominant direction over the next 12 hours (Figure 2c). The maximum tidal range observed over this experiment was ~ 1.5 m (Figure 2d). Currents with the reef system were relatively low before the passage of the storm event (Figure 2e-g) with current magnitudes typically between 0 and ~ 0.1 m s^{-1} . However, during the storm event, the currents significantly increased in magnitude with the flow out of North Passage (Figure 2g) reaching ~ 0.5 m s^{-1} .

3.2 Historical shoreline changes and sediment characteristics

The shoreline within the study area was found to be mostly stable (<10 m change in shoreline position over the ~ 60 year duration of the survey); however, there were also well-defined regions of accretion and erosion (Figure 3a). Significant accretion and erosion were considered to have occurred when the position of a section of shoreline had changed by more than 30 m over the survey duration. The greatest accretion occurred at Point Maud (~ 150 m, Figure 3b). Point Maud accreted consistently westward and grew most at the southern side of this cusped foreland. Between 1990 and 1995 the form of Point Maud became more rounded in shape and has remained approximately stable in form and position between 1995-2008. Both the southern and northern sides of Point Maud have also consistently accreted, although the northern side showed a period of erosion during the 1960's - 70's.

At Coral Bay Beach (Figure 3d), accretion was also observed and was greatest between 1949 and 1963. Since then the form of this section of coastline has remained approximately stable (<10 m change in shoreline position), with the exception of a period of erosion between 1969 and 1976. Between Point Maud and Coral Bay Beach, there is a region of erosion; however, this location has not always been associated with coastline erosion (Figure 3c). Between 1949 and 1983 the coastline at this location accreted by as much as ~ 50 m before the coastline began to erode and, based on the present data set, continues to erode.

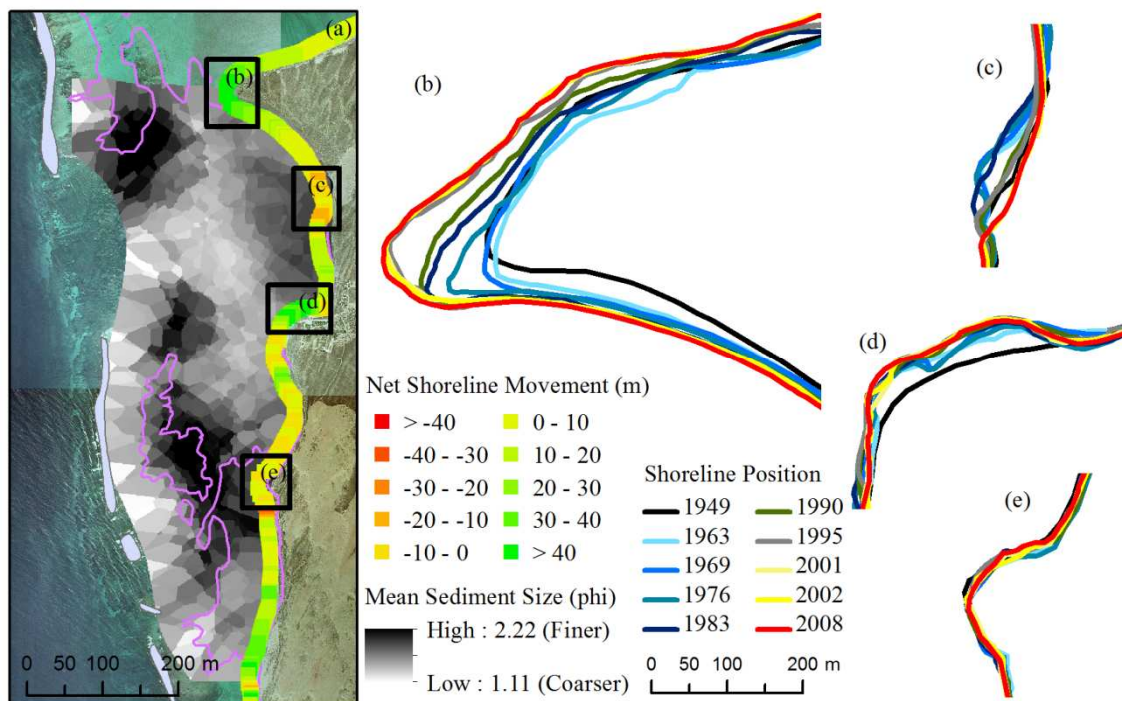


Figure 3. (a) Shoreline evolution along one part of the Ningaloo Reef coastline (red: erosion, green: accretion) and sediment size distribution at Coral Bay (July 2010). The reef crest is shaded in light grey and patches of sand amongst the coral communities are outlined in pink. The shoreline evolution (net shoreline movement) was measured as the change in shoreline position (m/year) from the most recent position (2008) compared to the original position (1949). Coastline position at (b) Point Maud, (c) between Point Maud and North Coral Bay (d) Coral Bay Beach and (e) Five Fingers.

The Five Fingers cusped foreland has remained in equilibrium and has experienced only minimal fluctuations in its coastline position (Figure 3e).

The sediment characteristics varied spatially around the site with the mean sediment size ranging from 1.1 - 2.2 Φ (Figure 3a), i.e. classified as medium grain sands. Finer sediments (2.2 – 1.8 Φ) were typically associated with un-colonized sandy regions whilst coarser sediments (1.1 – 1.3 Φ) were typically observed within areas of the reef dominated by coral communities (i.e., suggesting more recent biogenic production or that the hydrodynamic processes within the canopies are sufficient to transport finer sediments but not coarser sediments); however, this result was not always consistent. Three distinct regions of finer sediment were observed. The northern region (opposite Point Maud) was located slightly north of False Passage and behind the end of the reef crest north of the channel. A smaller region was located to the south of False Passage adjacent to North Coral Bay while a large region was located adjacent to Five Fingers and spanned a section of reef as well as a large patch of sandy bed. Medium grain sediment (1.6 – 1.7 Φ) was located close to the coastline within a coral community but adjacent to an erosive section of the coastline. The mean sediment size throughout the remainder of the region consisted of coarser medium grain sediment.

3.3 Circulation and bed shear stress distributions

The dissipation of incident swell waves on the forereef and reef crest consistently drives strong cross reef flows that circulate through the lagoons and return via channels to the ocean (Figure 4a). The flow at this site can be separated into two major circulation features:

The first are a series of “independent” reef circulation cells (Figure 4b), which are generated by flow over the reef that is partitioned in the lagoon and where the flow returns via a channel to the ocean. For this case, the hydrodynamic circulation within a reef-channel cell has minimal hydrodynamic connection with the adjacent regions of the reef. These classic wave-driven circulation features have been shown to occur in many other fringing reef sections, particularly those that are approximately parallel with the shoreline (e.g. Lowe et al., 2009; Taebi et al., 2011).

The second is an inter-connected hydrodynamic cell system (Figure 4c) where a wave-driven alongshore current is generated and propagates along the coastline in the lagoon between adjacent reef regions. For this circulation type, cross-reef flow is partitioned on the reef and in the lagoon with part of the flow converging with the alongshore current and the other part of the flow circulating near the reef and returning to the ocean via channels. This flow case occurs in the northern area of the study area where an alongshore current is generated adjacent to Five Fingers and travels northward through the system and finally exits into Bateman Bay near Point Maud. At Point Maud the convergence between the cross-reef flow and the alongshore current generates a strong north-easterly directed current which continues to travel along the coastline within Bateman Bay with decreasing magnitude. At the location near Point Maud where flow enters Bateman Bay, shear between the strong channel current and the water near the shoreline, which is shadowed by Point Maud, leads to the formation of a persistent clockwise eddy on the northern side of Point Maud.

A number of smaller-scale, localized circulation features are also observed in the circulation patterns and include: strong flow between the Five Fingers cusped foreland and the reef; eddies on the reef tips at the channel located in the southern reef cell; and two offshore eddies located in the channels located between Five Fingers and Coral Bay Beach (Figure 4a).

The estimated critical bed shear stress required to mobilize the sediment (Figure 5a) varied across the field experiment site, i.e. dependent on the sediment grain size ($\tau_{cr} = 0.16 - 0.25 \text{ N m}^{-2}$). The bed shear stress estimated by the numerical model under moderate wave conditions offshore (e.g. $H_{rms} = 1 \text{ m}$, $T_p = 14 \text{ s}$) was greater than the typical critical bed shear stress required to mobilize sediment over the reef flat (Figure 5b). This suggests that sediment produced on the reef flat (even coarse-grained sediment) can be mobilized and transported over the reef and into the lagoon, a process that explains the coarser sediment observed on the back reef (Figure 3a).

Within the lagoon, the bed shear stress imposed by the hydrodynamic conditions under the 1 m wave condition was considerably smaller (Figure 5b). This was caused by the attenuation of the incident waves due to the shallow reef crest ($\sim 0.6 - 1 \text{ m}$). Regions that consist almost exclusively of finer sediment experienced far less bed stresses than those regions covered by established coral communities. Adjacent to the Five Fingers cusp, enhanced flow due to the constriction between the reef and the cusped foreland,

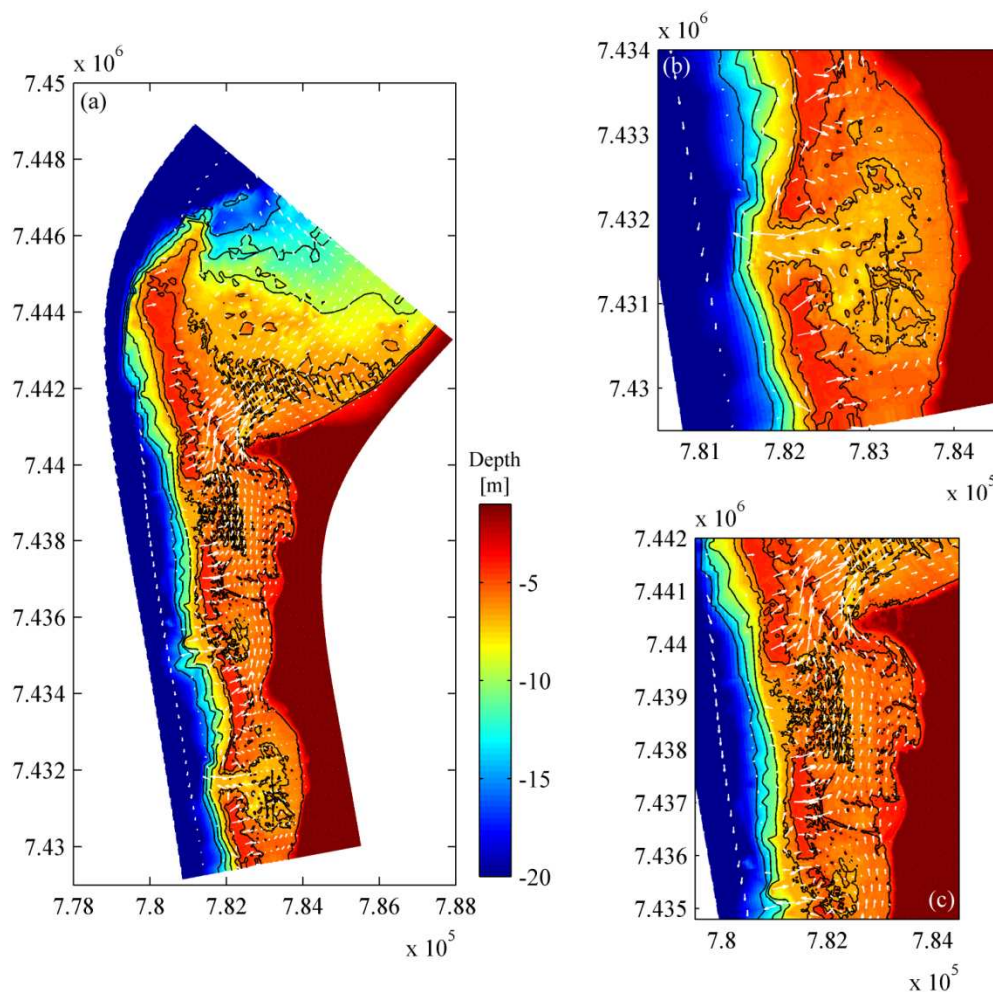


Figure 4. (a) Eulerian current velocity vectors for the whole domain (b) Higher resolution velocities for the southern half of the domain (c) Higher resolution velocities for the northern half of the domain. The vectors displayed in each figure have been plotted on a 10 m x 10 m vector scale.

combined with a narrow lagoon and greater wave propagation amplifies the shear stress at this location. Similarly, near Point Maud, established reef communities along with strong currents about Point Maud also generate high bed shear stresses. For higher wave conditions ($H_{rms} = 3.0$ m, $T_p = 14$ s), such as those that occurred during the storm in the field experiment, the bed shear stress across the entire reef and lagoon suggest that sediment will be mobilized over the majority of the domain (Figure 5c). The validity of this assessment is discussed further in Section 4.2.

4. Discussion

4.1 Coastline morphological formations

The Five Fingers cusped foreland is in an equilibrium state (at least since 1949). This suggests that the northward alongshore current inside the lagoon that accelerates between this protrusion and the reef flat is critical to the development and maintenance of this feature. It is conceptually proposed (Figure 6a) that this feature develops due to the transport of reef generated sediment across the lagoon which is then deposited at the shoreline due to (1) a reduction of wave-induced shear stress behind the reef and (2) a divergence in the cross reef flow, analogous to the mechanism proposed for the formation of shoreline features behind sand bars (Ranasinghe et al., 2004). However, as the cusped foreland develops and extends towards the

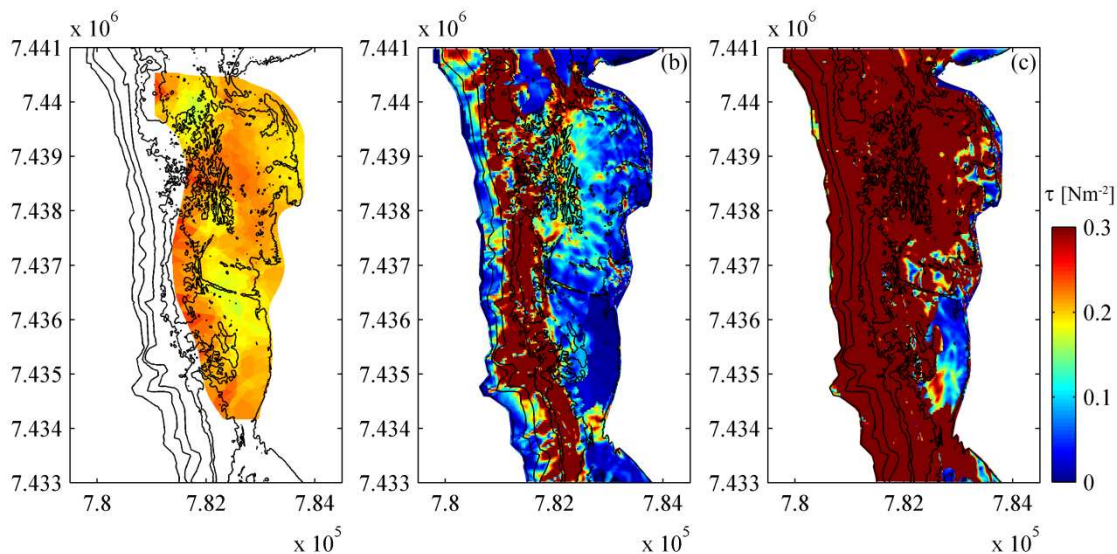


Figure 5. (a) The critical bed shear stress required to mobilize sediment based on the sediment grain size distributions. (b) The magnitude of the bed shear stress estimated by XBeach for moderate conditions ($H_{rms} = 1$ m, $T_p = 14$ s) (c) The magnitude of the bed shear stress estimated by XBeach for a storm condition ($H_{rms} = 3$ m, $T_p = 14$ s)

ocean, the alongshore current is accelerated due to the locally-constricted width of the lagoon (and supplemented by cross-reef flow) such that the bed shear increases (Figure 6b) hindering further accretion until a state of equilibrium is reached. This development is consistent with the presence of coarser material observed at the site slightly north of Five Fingers that may be transported by this accelerated current but would be deposited as the current decreases in magnitude outside the constriction. The circulation cell mechanism of salient development that has been observed behind offshore submerged breakwaters (Ranasinghe and Turner, 2006) was not observed in this study. This may be due to the geometrical differences associated with a natural offshore reef (wider, longer and further offshore) or that the development of an alongshore current in this region modifies the dominant hydrodynamics conditions at this site.

In contrast to the Five Fingers area, Point Maud was a much more dynamic feature during the study period. Whilst the tip of the cusped foreland appears to be in a state of equilibrium over the past decade (possibly for the same reasons as for Five Fingers), accretion along the northern and southern coasts was continuous with sediment eroded from the coast between North Coral Bay and Point Maud by alongshore currents and possibly wave action that propagates through False Passage during storm events. This sediment is transported along the coast by the current that is initially developed at Five Fingers then around the tip of Point Maud. Due to the high currents around this tip, sediment remains mobilized but eventually,

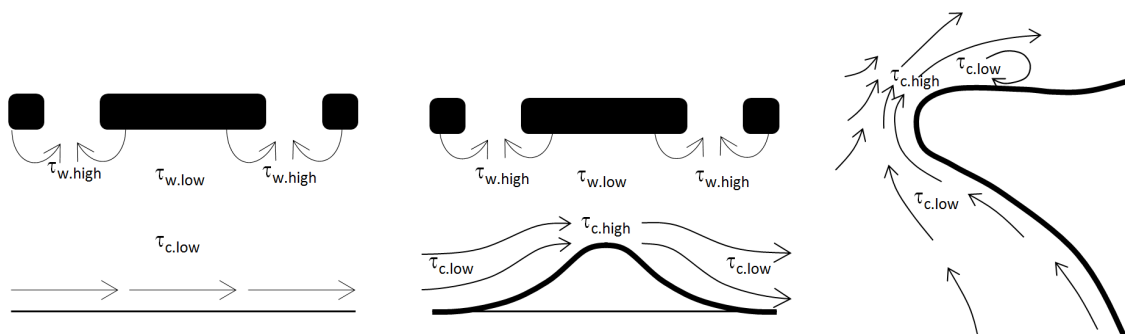


Figure 6. Conceptual feature development. (a) Dominant processes that result in the development of a cusped foreland (b) Change in bed shear stresses due to the development of the cusped foreland (c) Development of Point Maud by accelerated flow and a depositional eddy.

due to the decrease in current magnitude in Bateman Bay, sediment is deposited on the northern side of Point Maud (Figure 6c). Very low shear stress in the numerical model at the location of the circulation eddy (Figure 5c) is consistent with the entrapment and deposition of sediment in the conceptual model.

4.2 Applicability of bed shear stresses to estimates of sediment mobility

In this study (as well as all other historical reef sediment transport studies), the mobilization of sediment was inferred from bed shear stress driven by hydrodynamic processes (e.g. waves, currents), which describes the rate of momentum transfer to the seafloor. This approach is consistent with all sediment transport numerical models that use shear stresses computed from hydrodynamic models to determine the threshold of sediment motion. Ultimately this approach assumes that the stress exerted on a bed of sediment is equal and opposite to the stress that the overlying water column experiences. This is a valid assumption over a flat sandy surface where the flow can interact directly with sediments, but may result in an inaccurate estimation of the true bed stress experienced by sediment near the bottom of coral reef canopies.

In reef environments, momentum transfer (or the dissipation of hydrodynamic energy) can be dominated by the drag exerted by the reef canopies which is accounted for in hydrodynamic models with much higher friction coefficients (typically an order of magnitude or larger). Whilst this approach enables the 'correct' hydrodynamic bulk processes to be modeled, it may not correctly account for the fact that shear stresses acting on sediments embedded in reef canopies below the height of the roughness may be significantly reduced. For example, it has been shown that the velocity profile within the water column is modulated by the density and form of the coral community and that the near-bed orbital velocities can be considerably less than those at the top of the canopy (Lowe et al., 2005a; Lowe et al., 2005b; Rosman and Hench, 2011). As a consequence, the presence of high rugosity reef canopies has the potential to significantly modify the sediment deposition and re-suspension processes. Nevertheless, there is presently no practical way to describe sediment transport through such canopies.

Ultimately this implies that the true shear stresses exerted on sediments within and adjacent to reef canopies in this study will be lower than those predicted from the hydrodynamic model, thereby resulting in greater sediment stability and less sediment transport than predicted by our study – an important result if the purpose of the model is to understand sediment dynamics in a reef environment. This may explain why in this study, under storm conditions the critical bed shear stress is exceeded and that (theoretically) the entire bed should be mobilized, when in reality it may not in regions with dense coral reef assemblages.

5. Conclusion

The coastline fringed by Ningaloo Reef (Western Australia) from Point Anderson to Point Maud was found to be relatively stable, but with some well-defined regions of significant accretion and erosion. A large wave-driven alongshore current from Five Fingers to Bateman Bay that is generated and supported by cross reef flows is likely to play an important role in the transport of sediment northwards while also controlling coastline feature development via local flow accelerations between the hard coral reef and the accretionary shoreline cusped features. The sediment characteristics, particularly within the sandy regions of the site, are predicted by the model to remain stable under normal conditions but are likely to move within the coral communities under strong hydrodynamic conditions; however, there is uncertainty in these estimates due to effects that the large roughness will have on momentum dissipation and bed stresses within a reef canopy. Further research is therefore required in order to develop accurate but computationally efficient methods to address the complexities associated with sediment transport within reef structures.

Acknowledgements

This project forms part of a PhD study by A. Pomeroy at The University of Western Australia and is supported by a Robert and Maude Gledden Postgraduate Research Award, The Gowrie Trust Fund, a

University of Western Australia Postgraduate travel award and Deltares Strategic Funding in the framework of the “Event-driven hydro and morphodynamics” program. R. Lowe received support from an Australian Research Council Future Fellowship.

References

- Done, T. J. (1992), Phase shifts in coral reef communities and their ecological significance, *Hydrobiologia*, 247(1-3), 121-132.
- Gibbs, R. J., M. D. Matthews, and D. A. Link (1971), The relationship between sphere size and settling velocity, *Journal of Sedimentary Research*, 41(1), 7-18.
- Hardy, T. A., and I. R. Young (1996), Field study of wave attenuation on an offshore coral reef, *J. Geophys. Res.*, 101, 14311-14326.
- Lee, T. T., and K. P. Black (1978), The Energy Spectra of Surf Waves on a Coral Reef, *Coastal Eng*, 588-608.
- Lowe, R. J., J. Koseff, and S. G. Monismith (2005a), Oscillatory flow through submerged canopies: 1. Velocity structure, *J. Geophys. Res.*, 110, 1-17.
- Lowe, R. J., J. R. Koseff, and S. G. Monismith (2005b), Oscillatory flow through submerged canopies: 2. Canopy mass transfer, *J. Geophys.*, 110, 1-14.
- Lowe, R. J., J. L. Falter, S. G. Monismith, and M. J. Atkinson (2009), A numerical study of circulation in a coastal reef-lagoon system, *J. Geophys. Res.*, 114, C06022.
- Lowe, R. J., J. L. Falter, M. D. Bandet, G. Pawlak, M. J. Atkinson, S. G. Monismith, and J. R. Koseff (2005c), Spectral wave dissipation over a barrier reef, *J. Geophys. Res.*, 110, C04001.
- Monismith, S. G. (2007), Hydrodynamics of Coral Reefs, *Ann. Rev. Fluid. Mech.*, 39, 35-55.
- Moore, L. J. (2000), Shoreline mapping techniques, *Journal of Coastal Research*, 111-124.
- Ogston, A. S., C. D. Storlazzi, M. E. Field, and M. K. Presto (2004), Sediment resuspension and transport patterns on a fringing reef flat, Molokai, Hawaii, *Coral Reefs*.
- Perry, C. T., and L. J. Hepburn (2008), Syn-depositional alteration of coral reef framework through bioerosion, encrustation and cementation: Taphonomic signatures of reef accretion and reef depositional events, *Earth-Science Reviews*, 86(1-4), 106-144.
- Pomeroy, A. W. M., R. J. Lowe, G. Symonds, A. Van Dongeren, and C. Moore (2012), The dynamics of infragravity wave transformation over a fringing reef, *J. Geophys. Res.*
- Presto, M. K., A. S. Ogston, C. D. Storlazzi, and M. E. Field (2006), Temporal and spatial variability in the flow and dispersal of suspended-sediment on a fringing reef flat, Molokai, Hawaii, *Estuarine, Coastal and Shelf Science*, 67, 67-81.
- Ranasinghe, R., and I. L. Turner (2006), Shoreline response to submerged structures: A review, *Coastal Engineering*, 53(1), 65-79.
- Ranasinghe, R., G. Symonds, K. Black, and R. Holman (2004), Morphodynamics of intermediate beaches: a video imaging and numerical modelling study, *Coastal Engineering*, 51(7), 629-655.
- Roelvink, D., A. Reniers, A. van Dongeren, J. van Thiel de Vries, R. McCall, and J. Lescinski (2009), Modelling storm impacts on beaches, dunes and barrier islands, *Coastal Eng*, 56, 1133-1152.
- Rosman, J. H., and J. L. Hench (2011), A framework for understanding drag parameterizations for coral reefs, *J. Geophys. Res.*, 116(C8), C08025.
- Sanderson, P. G. (2000), A comparison of reef-protected environments in -Western Australia: the central west and Ningaloo coasts, *Earth Surface Processes and Landforms*, 25(4), 397-419.
- Sanderson, P. G., and I. Eliot (1996), Shoreline Salients, Cuspate Forelands and Tombolos on the Coast of Western Australia, *Journal of Coastal Research*, 12(3), 761-773.
- Scoffin, T. P. (1992), Taphonomy of coral reefs: a review, *Coral Reefs*, 11(2), 57-77.
- Soulsby, R., and R. Whitehouse (1997), Threshold of sediment motion in coastal environments, paper presented at Pacific Coasts and Ports' 97: Proceedings of the 13th Australasian Coastal and Ocean Engineering Conference and the 6th Australasian Port and Harbour Conference; Volume 1, Centre for Advanced Engineering, University of Canterbury.
- Storlazzi, C. D., A. S. Ogston, M. H. Bothner, M. E. Field, and M. K. Presto (2004), Wave- and tidally-driven flow and sediment flux across a fringing coral reef: Southern Molokai, Hawaii, *Continental Shelf Research*, 24, 1397-1419.
- Taebi, S., R. J. Lowe, C. B. Pattiaratchi, G. N. Ivey, G. Symonds, and R. Brinkman (2011), Nearshore circulation in a

- tropical fringing reef system, *J. Geophys. Res.*, *116*, C02016.
- Thieler, E., E. Himmeltoss, J. Zichichi, and E. Ayhan (2008), Digital Shoreline Analysis System (DSAS) version 4.0 - An ArcGIS extension for calculating shoreline change *Rep. 1278*, US Geological Survey.
- Van Dongeren, A., R. Lowe, A. Pomeroy, D. M. Trang, D. Roelvink, G. Symonds, and R. Ranasinghe (2013), Numerical modeling of low-frequency wave dynamics over a fringing coral reef.
- Vecsei, A. (2004), A new estimate of global reefal carbonate production including the fore-reefs, *Global and Planetary Change*, *43*(1-2), 1-18.
- Wyatt, A. S. J., R. J. Lowe, S. Humphries, and A. M. Waite (2010), Particulate nutrient fluxes over a fringing coral reef: relevant scales of phytoplankton production and mechanisms of supply, *Marine Ecology Progress Series*, *405*, 113-130.
- Young, I. R. (1989), Wave Transformation Over Coral Reefs, *J. Geophys. Res.*, *94*, 9779-9789.
- Zhang, Z., J. Falter, R. Lowe, and G. Ivey (2012), The combined influence of hydrodynamic forcing and calcification on the spatial distribution of alkalinity in a coral reef system, *Journal of Geophysical Research*, *117*(C4), C04034.